RESEARCH ARTICLE

Figures and figure supplements

A prefrontal-bed nucleus of the stria terminalis circuit limits fear to uncertain threat

Lucas R Glover *et al*

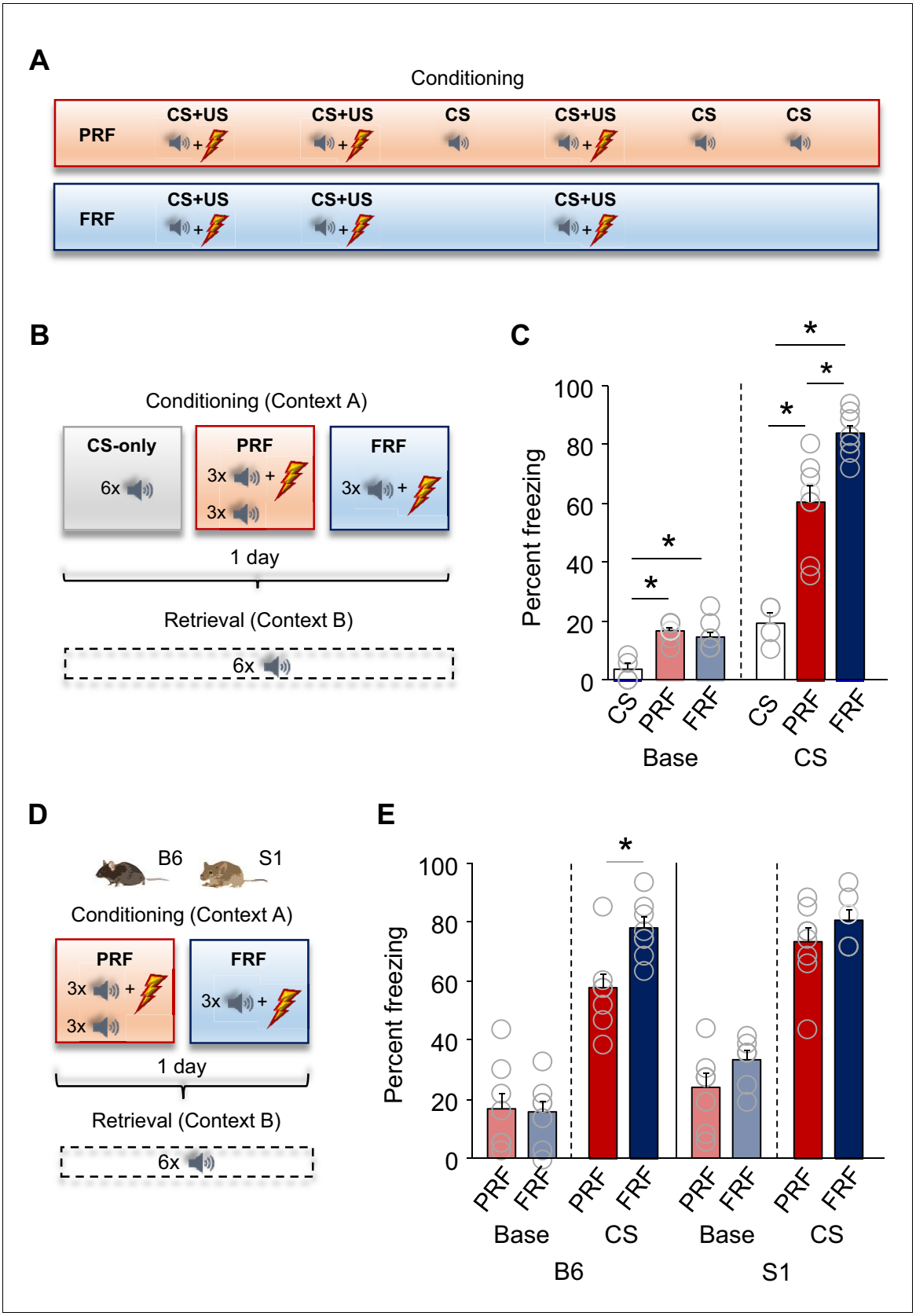

Figure 1. Lower freezing during retrieval of partially reinforced fear; effects of genetic strain. (**A**) Schematic depiction of experimental procedure for assessing, in B6 mice, PRF and FRF, along with CS-only controls. (**B**) Schematic depiction of experimental procedure for assessing, in B6 mice, PRF and

Figure 1 continued on next page

Figure 1 continued

FRF retrieval in a novel context (context B) and the conditioning context (context A) (C) Lower CS-related freezing during retrieval in PRF mice than in FRF mice. Higher baseline and CS-related freezing in PRF and FRF mice relative to CS-only controls (n = 4–8 mice per group). (**D**) Schematic depiction of experimental procedure for assessing PRF and FRF retrieval in the B6 and S1 genetic strains. (E) Lower CS-related freezing during retrieval in PRF than in FRF in B6, not S1, mice (n = 7–8 mice per group/strain). Data are means ± SEM. *p<0.05.

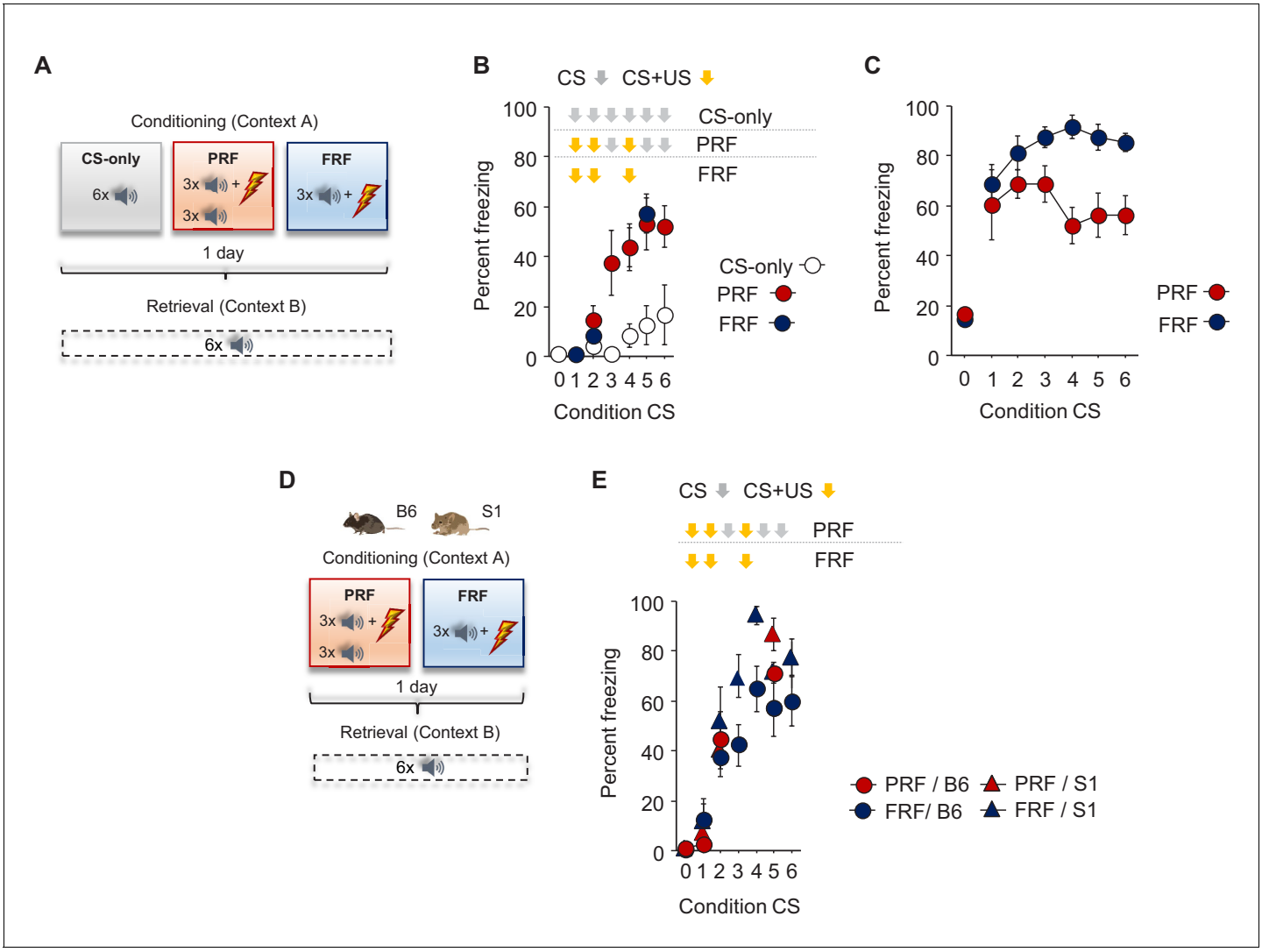

Figure 1—figure supplement 1. Freezing during conditioning. (**A**) Schematic depiction of experimental procedure for assessing, in B6 mice, PRF and FRF, along with CS-only controls. (**B**) No group differences in CS-related freezing during conditioning (n = 4–8 mice per group). (**C**) No difference in CS-related freezing between FRF and PRF mice during retrieval, broken down by CS presentation (n = 8 mice per group). (**D**) Schematic depiction of experimental procedure for assessing PRF and FRF retrieval in the B6 and S1 genetic strains. (**E**) No group differences in CS-related freezing during conditioning (n = 7–8 mice per group/strain). Data are means ± SEM.

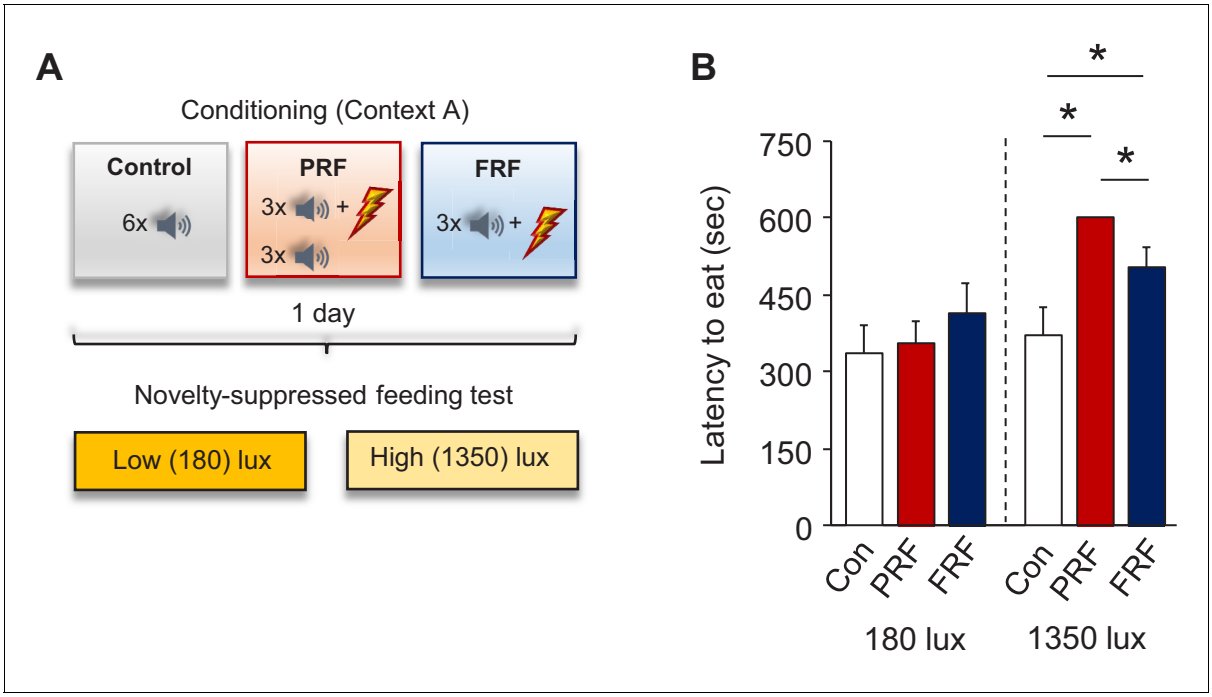

Figure 1—figure supplement 2. Increased latency to feed in the NSF test after PRF. (**A**) Schematic depiction of experimental procedure for assessing behavior on the novelty-suppressed feeding (NSF) test after PRF or FRF conditioning, along with context-exposed controls. (**B**) Longer latencies to eat under high, but not low, illumination in PRF and FRF versus controls and in PRF versus FRF. n = 8 mice per group. Data are means ± SEM. *p<0.05.

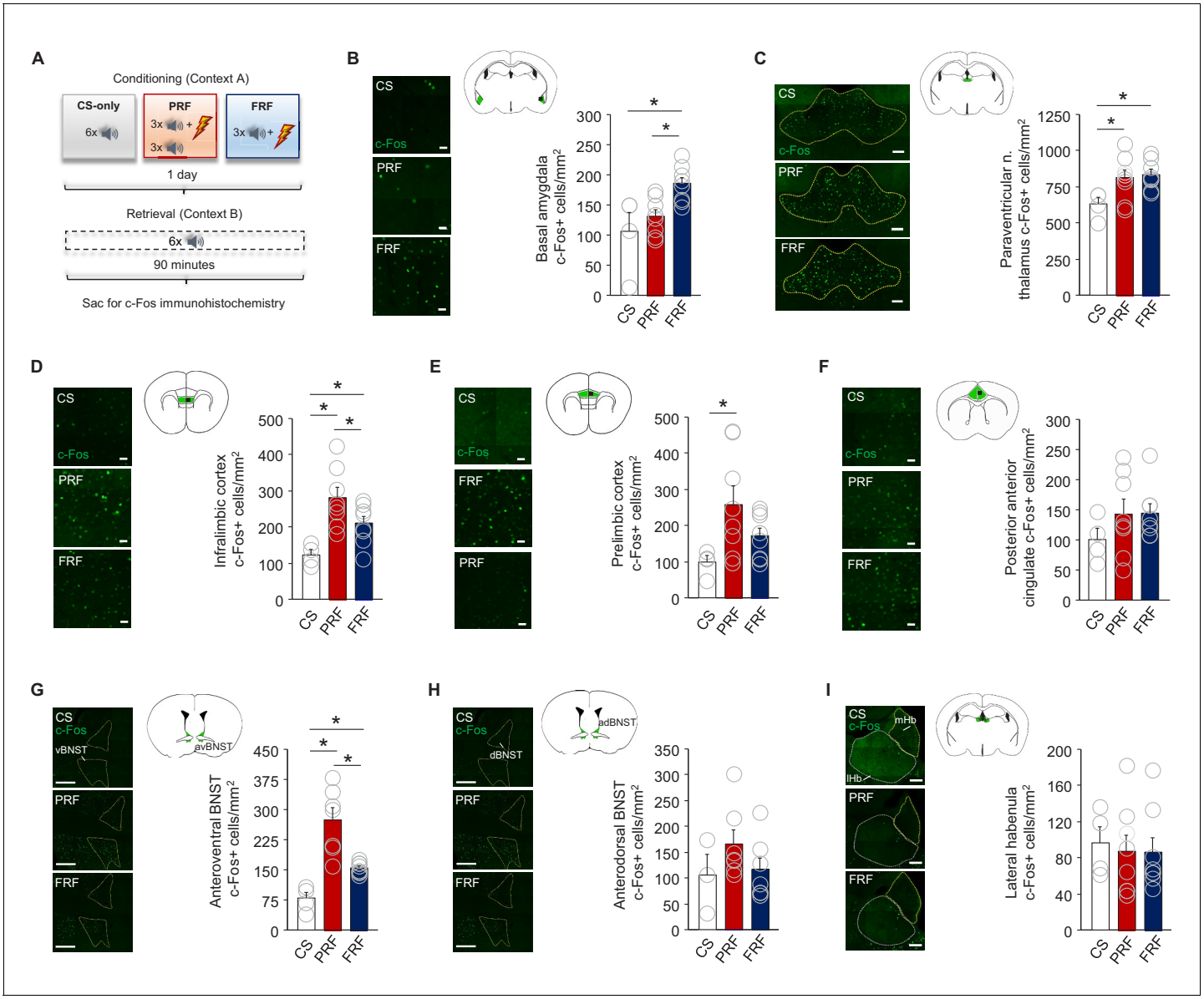

Figure 2. PRF preferentially activates subregions of mPFC and BNST. (**A**) Schematic depiction of experimental procedure for assessing ex vivo neuronal regional activity (via c-Fos immunohistochemistry) after PRF or FRF retrieval, along with CS-only controls. Representative images and c-Fos+ cell count differences for basal amygdala (**B**), paraventricular nucleus of the thalamus (**C**), infralimbic cortex (**D**), prelimbic cortex (**E**), posterior portion of the anterior cingulate cortex (**F**), anteroventral BNST (**G**), anterodorsal BNST (**H**), and lateral habenula (**I**). For corresponding behavioral data, see ***Figure 1B***. Scale bars = 30 μm (**B,D–F**), 100 μm (**C,I**), 300 μm (**G,H**). n = 4–8 mice per group. Data are means ± SEM. *p<0.05.

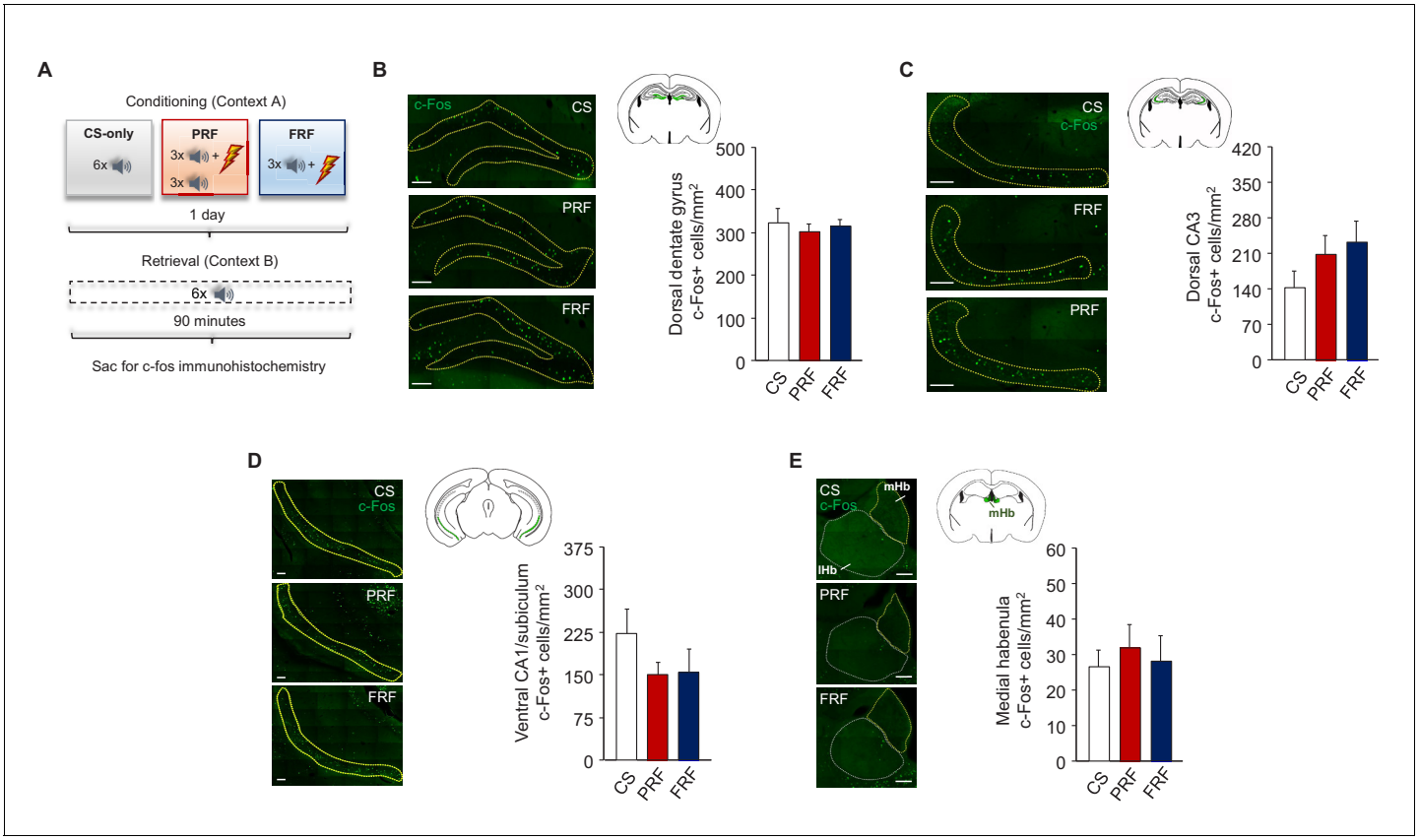

Figure 2—figure supplement 1. Ex vivo neuronal regional activity correlates of PRF. (**A**) Schematic depiction of experimental procedure for assessing ex vivo neuronal regional activity (via c-Fos immunohistochemistry) after PRF or FRF retrieval. Representative images and c-Fos+ cell counts for the dorsal dentate gyrus (**B**), dorsal CA3 (**C**), and ventral CA1/subiculum (**D**) regions of the hippocampus and the medial habenula (**E**). There were no group differences. Scale bars = 100 μm. n = 4–8 mice per group. Data are means ± SEM.

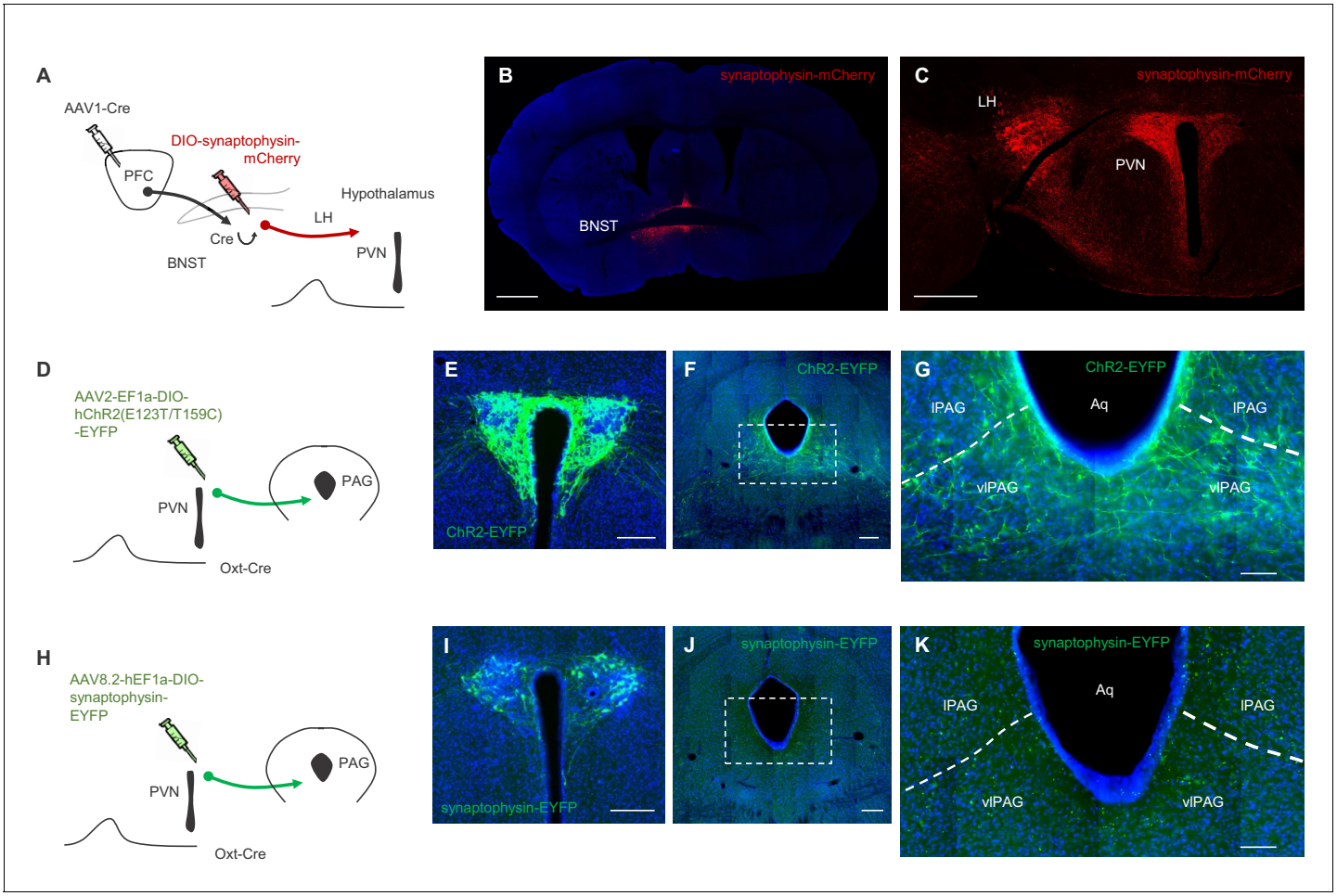

Figure 2—figure supplement 2. Connectivity between mPFC, BNST, and downstream targets. (**A**) Schematic depiction of viral strategy to label mPFC inputs to BNST neurons and their onward projections to the hypothalamus. (**B**) Representative image of synaptophysin-mCherry labeling in BNST neurons receiving mPFC input (scale bar = 1000 μm). (**C**) Representative image of synaptophysin-mCherry labeling in mPFC-innervated BNST neuronal projections in hypothalamus (scale bar = 500 μm). (**D**) Schematic depiction of viral strategy to label PVN oxytocin cell inputs to the PAG in Oxt-Cre mice. (**E**) Representative image of ChR2-EYFP labeling in the PVN (scale bar = 200 μm). Low (**F**) and high (**G**) magnification images of ChR2-EYFP labeling in the PAG (scale bars = 200 μm and 100 μm, respectively). (**H**) Schematic depiction of viral strategy to label PVN oxytocin cell inputs to the PAG in Oxt-Cre mice. (**I**) Representative image of synaptophysin-EYFP labeling in the PVN (scale bar = 200 μm). Low (**J**) and high (K) magnification images of synaptophysin-EYFP labeling in the PAG (scale bars = 200 μm and 100 μm, respectively). Note: LH = Lateral Hypothalamus; PVN = paraventricular nucleus of the hypothalamus; lPAG = lateral periaqueductal gray; vlPAG = ventrolateral periaqueductal gray; Aq = aqueduct.

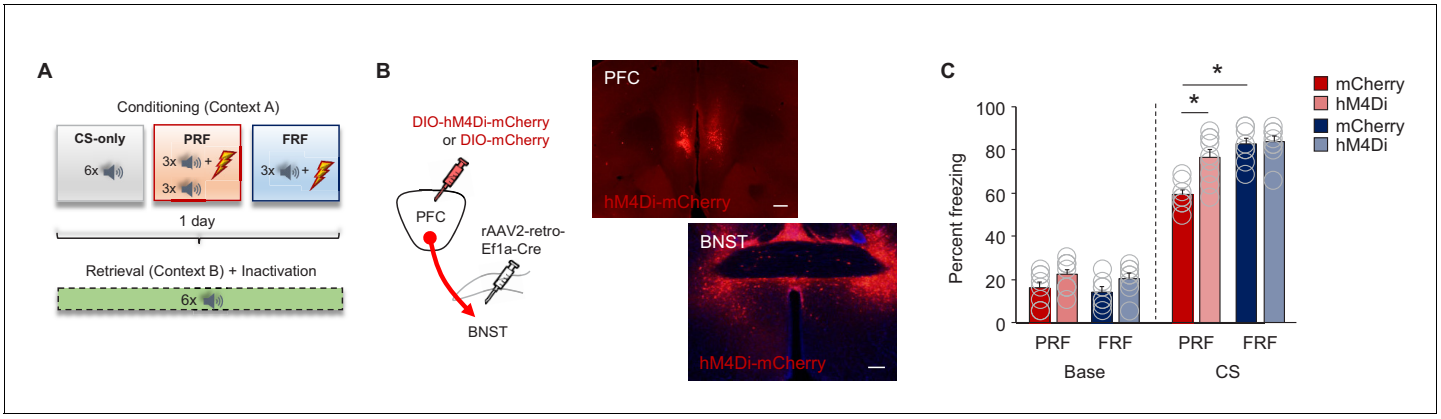

Figure 3. Inhibition of mPFC→BNST neurons increases PRF. (**A**) Schematic depiction of experimental procedure for assessing effects of chemogenetic inhibition of mPFC→BNST neurons during retrieval. (**B**) Cartoon of viral strategy and representative images of hM4Di–mCherry labeling in BNST neurons receiving mPFC input (scale bars = 200 μm). (**C**) Lower CS-related freezing during retrieval in PRF mice than in FRF mice transfected with mCherry, not hHM4Di. Data are means ± SEM. *p<0.05.

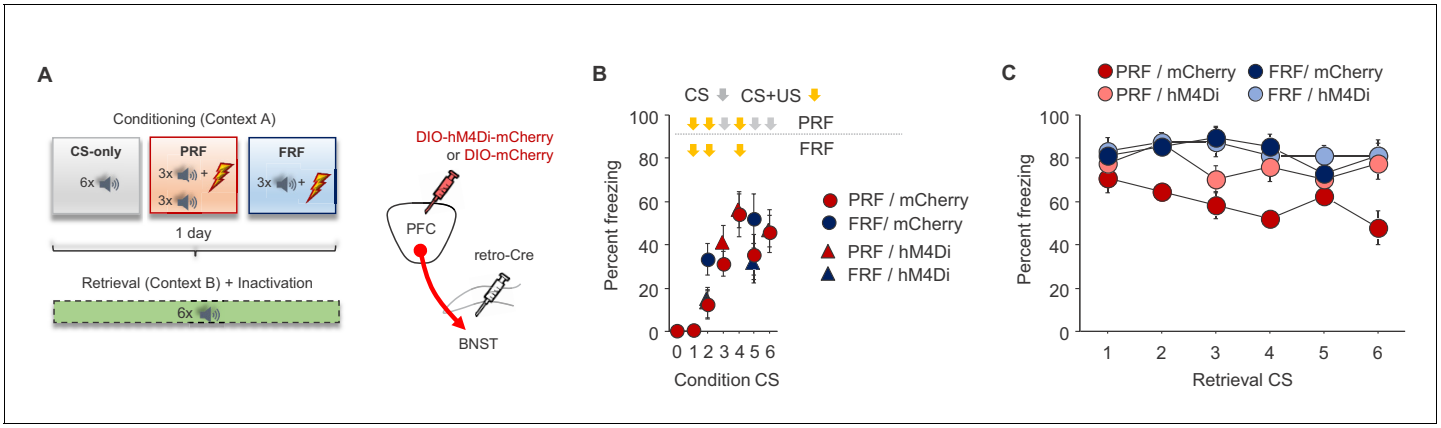

Figure 3—figure supplement 1. Freezing during conditioning prior to mPFC→BNST inhibition on retrieval. (**A**) Schematic depiction of viral strategy to selectively inhibit BNST-projecting mPFC neurons during retrieval. (**B**) Freezing increased across CS trials, irrespective of virus group. (**C**) Trial-by-trial breakdown of freezing during each CS of retrieval indicated a non-significant trend for decreasing freezing across trials in the mCherry PRF group. n = 8–9 mice group/virus. Freezing data are means ± SEM.

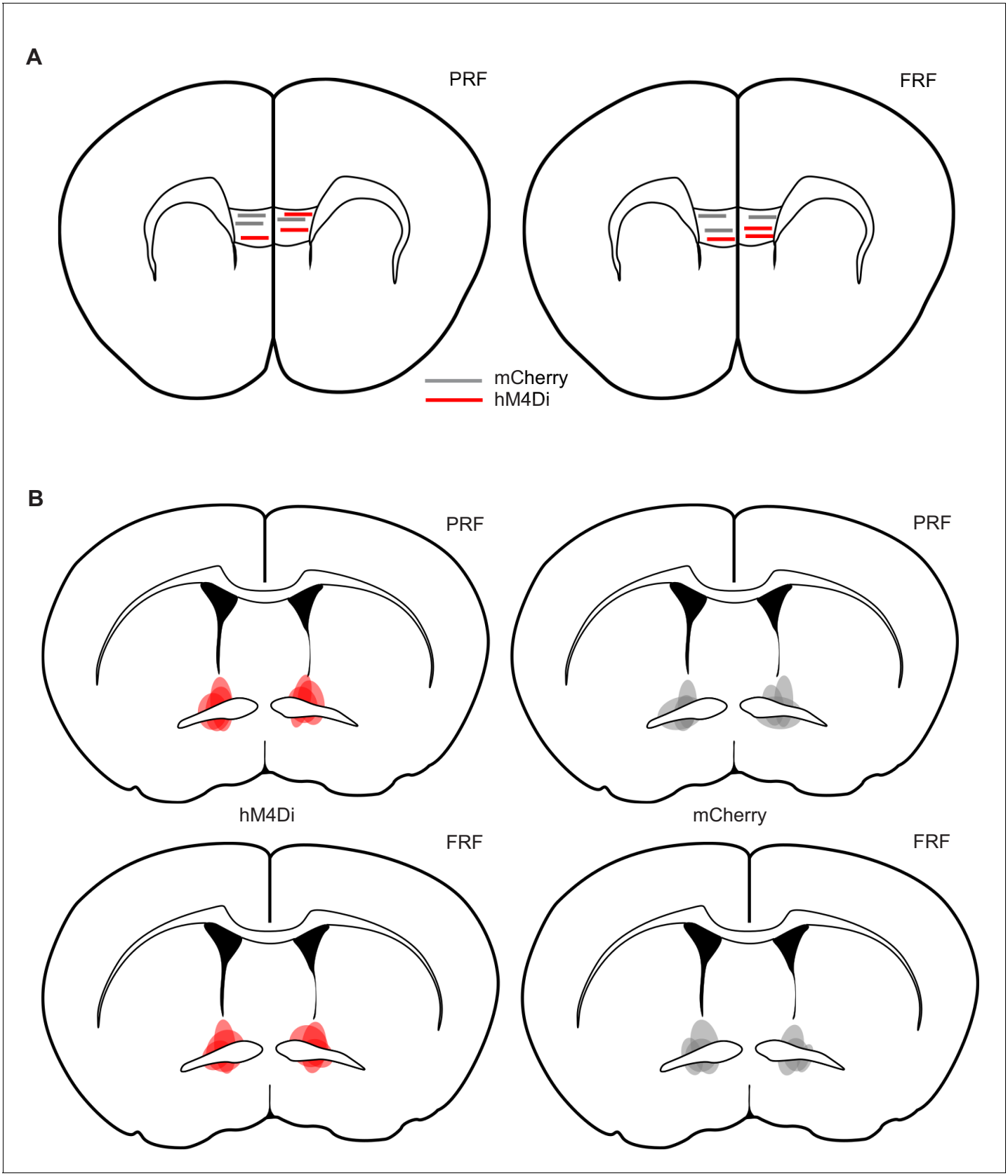
A
PRF
FRF
mCherry
hM4Di
B
PRF
PRF
hM4Di
mCherry
FRF
FRF

Figure 3—figure supplement 2. Electrode placements and virus localization for combined chemogenetic/single-unit recordings. Estimated location of tips of the electrodes at the center of the multi-array in the IL of PRF (**A**) and FRF (**B**) mice. Estimated extent of virus, as indicated by mCherry expression, in the BNST of PRF (**C**) and FRF (**D**) mice (darker shading represents areas of greater overlap across mice).

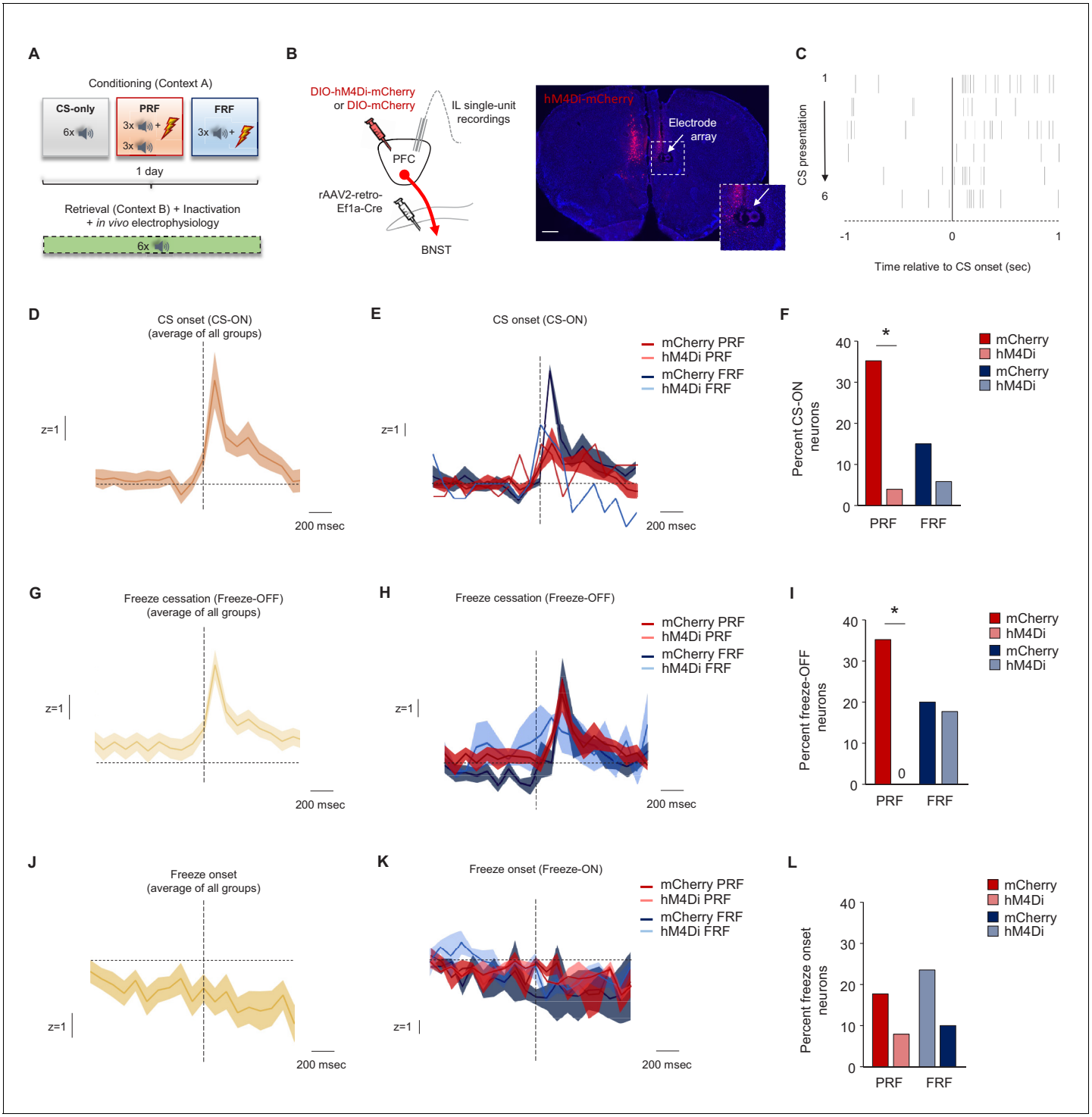

Figure 3—figure supplement 3. CS and freezing-related IL unit activity and effects of mPFC→BNST inhibition. (**A**) Schematic depiction of experimental procedure for in vivo IL single-unit recordings, combined with chemogenetic inhibition of mPFC→BNST neurons during retrieval (n = 8–9 mice per group/virus). (**B**) Cartoon of viral strategy and representative image of hM4Di-mCherry labeling in the mPFC and electrode array placement in the IL (scale bar = 500 µm). (**C**) Raster plot of a representative IL unit firing in response to CS onset (CS-ON neuron). Baseline-normalized population trace of CS-ON neuronal activity during retrieval; average of all groups (**D**) and split by group (**E**). (**F**) Higher percentage of CS-ON units during PRF than FRF retrieval in mice transfected with mCherry, not hHM4Di (n = 17 recorded units in PRF/mCherry, n = 25 units in PRF/hM4Di, n = 20 units in FRF/mCherry, n = 17 units in FRF/hM4Di, from three mice per group/virus). Baseline-normalized population trace of freeze cessation (Freeze-OFF neurons) IL unit activity during retrieval; average of all groups (**G**) and split by group (**H**) (n = 3 CS units in PRF/mCherry, n = 6 units in PRF/hM4Di, n = 1 units in

Figure 3—figure supplement 3 continued on next page

Figure 3—figure supplement 3 continued

FRF/mCherry, n = 1 units in FRF/hM4Di). (**I**) Higher percentage of Freeze-OFF units during PRF than FRF retrieval in mice transfected with mCherry, not hHM4Di (n = 17 recorded units in PRF/mCherry, n = 25 units in PRF/hM4Di, n = 20 units in FRF/mCherry, n = 17 units in FRF/hM4Di, from three mice per group/virus, n = 4 Freeze-OFF units in PRF/mCherry, n = 6 units in PRF/hM4Di, n = 3 units in FRF/mCherry, n = 0 units in FRF/hM4Di). Baseline-normalized population trace of freeze onset (Freeze-ON neurons) IL unit activity during retrieval; average of all groups (**J**) and split by group (**K**). (**L**) No differences in the percentage of Freeze-OFF units during retrieval between groups (n = 17 units in PRF/mCherry, n = 25 units in PRF/hM4Di, n = 20 units in FRF/mCherry, n = 17 units in FRF/hM4Di, from three mice per group/virus, n = 4 Freeze-ON units in PRF/mCherry, n = 6 units in PRF/hM4Di, n = 4 units in FRF/mCherry, n = 2 units in FRF/hM4Di). Data are means ± SEM. *p<0.05.

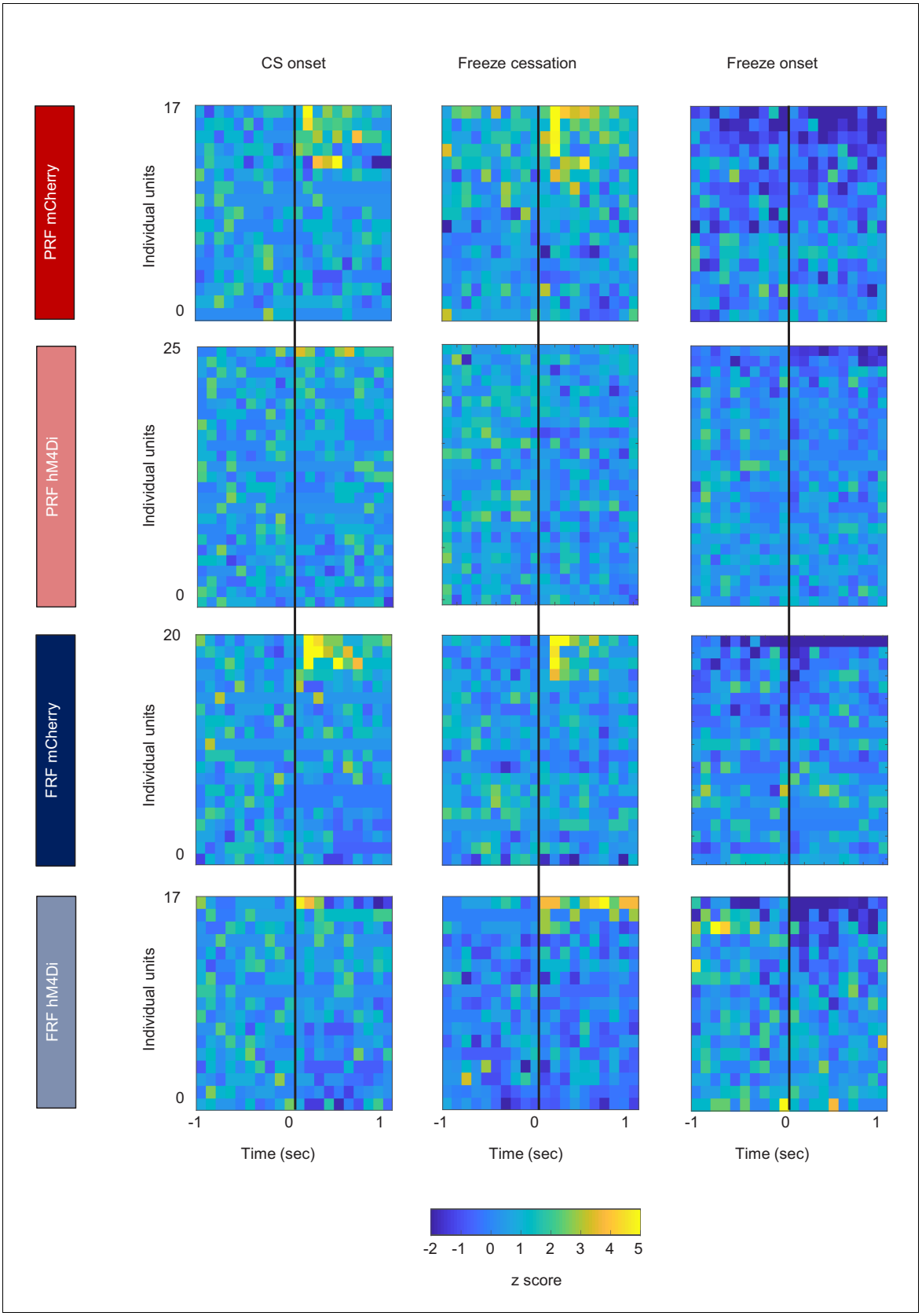
CS onset
Freeze cessation
Freeze onset
PRF mCherry
PRF hM4Di
FRF mCherry
FRF hM4Di
Individual units
17
0
25
0
20
0
17
0
-1
0
1
Time (sec)
-2 -1 0 1 2 3 4 5
z score

Figure 3—figure supplement 4. Heat maps illustrating IL unit activity. (A) Heat plots of unit activity aligned to CS onset (left columns), freeze cessation (center columns), and freeze onset (right columns). The same data shown as peri-event histograms and % event-related activity can be found in ***Figure 3—figure supplement 3***.